

Article

Reappraising a Controversy: Formation and Role of the Azodication (ABTS²⁺) in the Laccase-ABTS Catalyzed Breakdown of Lignin

Gerhard Gramss

Institute of Earth Sciences, Friedrich-Schiller-University, Burgweg 11, D-07749 Jena, Germany; gerhard.gramss@uni-jena.de

Academic Editors: Thaddeus Ezeji and Mohammad J. Taherzadeh

Received: 11 May 2017; Accepted: 8 June 2017; Published: 15 June 2017

Abstract: In fermentations of lignocelluloses, redox potentials (If not indicated otherwise, redox potentials in Volt are taken versus Normal Hydrogen Reference Electrodes (NHE).) E^0 of laccases/plant peroxidases by 0.79/0.95 V enable oxidations of phenolic substrates and transformations of synthetic and substrate-derived compounds to radicals that mediate attacks on non-phenolic lignin (models) by 1.5 V. In consecutive one-electron abstractions, the redox mediator 2,2'-azinobis-(3-ethylbenzothiazoline-6-sulfonate) (ABTS) is oxidized by electro- or wet-chemistry to the green cation radical (ABTS^{•+}, 0.68 V) and the red dication (ABTS²⁺, 1.09 V). The enzyme/ABTS couple generates the stable ABTS^{•+} whose low E^0 cannot explain the couple's contemporary attack on non-phenolic lignins. This paradoxon indicates the non-confirmed production of the ligninolytic ABTS²⁺ by the enzymes. During incubations of live sapwood chips in ABTS/H₂O₂ to prove their constitutive peroxidase, the enzyme catalyzed the formation of the expected green-colored ABTS^{•+} solution that gradually turned red. Its spectrophotometric absorbance peaks at $\lambda = 515\text{--}573$ nm resembled those of ABTS²⁺ at 518–520 nm. It is shown that portions of an ABTS^{•+} preparation with inactivated enzyme are reduced to ABTS during their abiotic oxidation of low-MW extractives from lignocelluloses to redox mediating radicals. The radicals, in turn, apparently transform the remaining ABTS^{•+} to red derivatives in the absence of functional oxidoreductases. Ultrafiltration and Liquid-Chromatography suggest the presence of a stable ABTS²⁺ compound absorbing at 515 nm, red protein/ABTS adducts, and further ABTS moieties. Therefore, ABTS mediated lignin degradations could result from chain reactions of ABTS^{•+}-activated lignocellulose extractives and fissured rather than complete ABTS²⁺ molecules.

Keywords: laccase; plant peroxidase; redox mediator; ABTS dication; lignin degradation; wood extractives

1. Introduction

The recalcitrant plant lignins form 5%, 11%, and 27% of the dry biomass of ryegrass, alfalfa [1] and Norway spruce timber, respectively [2]. In the lignocellulose scaffold of wheat straw, portions of 11–23% lignin [3–5] protect the crystalline cellulose fibrils (33–40%) and hemicelluloses (21–26%) from microbial decay by the formation of intimate structural links [6,7]. Lignin degradation is apparently catalyzed by the joint action of endo- and exooxygenases and oxidoreductases such as laccases and peroxidases of plants; white-rot, soft-rot, and brown-rot fungi; and bacteria [8–10]. The enzymes operate in concert with low-MW carboxylic acids, reactive oxygen species, transition metal cations, and small organic radical molecules of substrate or metabolic origin which are referred to as redox mediators [11–14]. They mediate electron abstractions from substrates whose electron withholding capacity (E^0) surpasses the redox potential of the enzyme itself.

Exploiting selective delignifications, especially by laccases, is the primary goal of the chemical kraft pulp refining in the paper industry [15,16]. Current working protocols of the lignocellulose feedstock for bioethanol production recommend laccases for the detoxification of furans and phenols as fermentation inhibitors in the pre-treated pulp rather than for early delignification steps [17,18]. Initial one-electron oxidations of the dominating non-phenolic lignin units presuppose redox potentials of $E^0 > 1.5$ V [16]. This catalytic potential is afforded by lignin peroxidases and versatile peroxidases in combination with the electron acceptor H_2O_2 in vitro ($E^0 = 1.4$ – 1.5 V) (see [8,12,19–21] for reviews). Manganese dependent peroxidases of basidiomycete fungi complete their redox cycle by the oxidation of two Mn^{2+} cations to the abiotic oxidant Mn^{3+} ($E^0 = 0.8$ – 0.9 V for Mn^{3+} /malonate or oxalate complexes) [21,22]. The cation performs one-electron abstractions from phenolic substrate molecules or phenolic lignin structures [23,24] upon its reduction to Mn^{2+} and is enzymatically reoxidized to Mn^{3+} by electron transfer to H_2O_2 . Laccases of basidiomycetes (E^0 up to 0.79 V) catalyze one-electron abstractions from hydroxyl groups of four phenolic molecules (up to 0.81 V) [25] to convert the electron acceptor O_2 to two H_2O . They initiate oxidations, decarboxylations, demethylations, and demethoxylations from phenolic acids (derivatives) and phenolic lignin moieties. The resulting aryloxy radicals polymerize or depolymerize to low-MW mediators to initiate spontaneous C_α - C_β bond cleavages, C_α oxidations, and alkyl-aryl and aromatic ring cleavages in phenolic lignin model compounds [26,27]. Laccase/synthetic mediator systems (E^0 up to 1.5 V) oxidize the lignin model surrogate veratryl alcohol ($E^0 = 1.4$ V) and nonphenolic structures of lignin model compounds [28–31].

More than 100 low-MW fungal metabolites, substrate breakdown moieties, and synthetic compounds have been tested for their ability to expand the substrate range of the oxidoreductases as above to the recalcitrant structures of lignin, dyes, and anthropogenic xenobiotics such as polycyclic aromatic hydrocarbons (e.g., [12,14,32–35]). Although (plant) peroxidases and laccases are with molecular sizes of 34–70 kDa in the 4.5–8.5 nm range (horseradish peroxidase C = 4 nm) and face lignin molecules that exceed several 100 nm [36], the enzyme molecules fail to penetrate into the lignified cell walls where breakdown occurs. Consequently, the actual in situ catalytic performance is being ascribed to the small diffusible radicals of redox mediators and intermediate metabolites (e.g., [37]). In practice, combinations of the common oxidoreductases with the preferred synthetic compounds 1-hydroxybenzotriazole (HBT, $E^0 = 1.08$ V) and 2,2'-azinobis-(3-ethylbenzothiazoline-6-sulfonate) (ABTS) support the catalytic conversion processes significantly [37,38]. In two consecutive one-electron abstractions, the colorless ABTS molecule is oxidized to the green ABTS cation radical ($ABTS^{\bullet+}$) and the red colored ABTS dication or azodication ($ABTS^{2+}$, Figure 1). The last color change is due to the formation of the chromogenic $-N=N-$ azo group and its interaction with the adjacent molecular structures [39]. The oxidation/reduction steps can be performed electrochemically by cyclic voltammetry. Dissolved in a buffer solution, ABTS is exposed to rising and falling electrical potentials of -600 to 1200 mV erected between counter and reference electrode (commonly Ag/AgCl) to reveal the voltages (redox potentials) that correspond with the oxidation and reduction steps [29,40,41].

In wet-chemistry, $ABTS^{2+}$ forms with an excess of the oxidant under strongly acidic conditions [42,43]. Among the abiotic oxidants of ABTS, MnO_4^- , $Cr_2O_7^{2-}$, and Cr(IV) generated the red dication. Its rapid decay was delayed by $S_2O_8^{2-}$ for more than three days [44]. Among inorganic peroxides generating the $ABTS^{\bullet+}$ cation radical, peroxodisulfate alone produced the dication [45]. A stable but floccose red-brown product precipitated from ABTS solution of pH 2 in the presence of potassium peroxodisulfate ($K_2O_8S_2$, $E^0 = 2.01$ V). It was re-dissolved by electron partition with equimolar ABTS supplements in a comproportionation reaction to the green $ABTS^{\bullet+}$ solution [46].

The redox potentials E^0 for the oxidation steps ABTS to $ABTS^{\bullet+}$ and $ABTS^{\bullet+}$ to $ABTS^{2+}$ amounted 472 and 885 mV, respectively [29], and were re-determined with 477 ± 1.2 and 933.6 ± 3.7 mV, respectively, against Ag/AgCl reference electrodes [47], independent of pH [48]. Values of 0.68 and 1.09 V, respectively, were obtained against the Normal Hydrogen Electrode (NHE; Figure 1) [41]. The electrochemically generated green $ABTS^{\bullet+}$ shows spectrophotometric absorbance peaks at $\lambda = 417, 645,$

728, and 810 nm in the visible light spectrum [41]. ABTS^{2+} has a single peak at $\lambda = 518\text{--}520$ nm [30,41,45] and an extinction coefficient $\epsilon_{518} = 36,000 \text{ M}^{-1} \text{ cm}^{-1}$ [41].

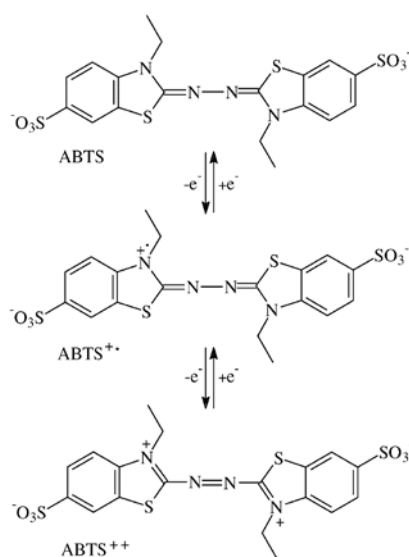


Figure 1. Oxidation of the heterocyclic ABTS molecule (shown as a dianion) to ABTS^{2+} by two consecutive electron abstractions.

In their role as one-electron oxidants, $\text{ABTS}^{•+}$ was confined to phenolic substrates, whereas the electrochemically generated ABTS^{2+} was able to oxidize veratryl alcohol ($E^0 = 1.4$ V) and non-phenolic aromatics [29,30]. As these reactions are also catalyzed by cell-free laccase/ABTS systems [46,49,50], they could point to the hitherto non-confirmed production of ABTS^{2+} by pure laccase. While laccases transform ABTS to the stable green $\text{ABTS}^{•+}$ cation radical, its further unambiguous oxidation to the dication was not shown [28,30,51]. Nevertheless, details of the reaction kinetics [52], pH dependence [53], patterns and catalytic potentials of substrate conversion [29,46] and presence of graphene [54] suggest contributions of ABTS^{2+} to the laccase/ABTS catalysis.

The manganese independent class III peroxidase represented by a set of isoforms [55] is constitutive to all terrestrial plants. Peroxidases are involved in lignification, cell elongation, stress response, and seed germination [56]. They have redox potentials of 0.89–0.95 V [19], oxidize phenolics up to 1.12 V [25], and are potential laccase substitutes in biotechnology [12,55]. Screenings for peroxidase activity were performed across the stemwood regions of European trees with wood chips incubated in ABTS/ H_2O_2 reaction mixtures (unpublished). To the surprise, the normally stable green $\text{ABTS}^{•+}$ solutions formed within 10–60 min were further oxidized and acquired red to brownish tones within 0.5–8 (–24) h. The spectrophotometric absorbance peaks of $\text{ABTS}^{•+}$ were replaced by single ones that resembled those reported for the red colored ABTS^{2+} [30,45].

In this study, the production of the reddish ABTS derivatives was followed in ABTS solutions amended with wood chips, wheat straw, and green stem sections of grass. It was the goal to identify extractives of the respective plant tissues in their role as ubiquitous natural redox mediators and to characterize the ABTS derivatives by Liquid Chromatography, ultrafiltration, and UV-Vis and FT-IR spectrophotometry in partial comparison with an ABTS^{2+} product generated with the oxidant $\text{K}_2\text{O}_8\text{S}_2$. Consequences for ABTS applications in biotechnology are discussed.

2. Materials and Methods

2.1. Preparation of Sapwood Chips

Chips from the outer sapwood of vital branches \varnothing 12–20 mm were taken from two to three accessions each of the tree species European beech (*Fagus sylvatica* L.); sycamore (*Acer pseudoplatanus*

L.); European birch (*Betula verrucosa* Ehrh.); common oak (*Quercus robur* L.); hornbeam (*Carpinus betulus* L.); Norway spruce (*Picea abies* [L.] Karst.); and Scots pine (*Pinus sylvestris* L.). Tangential chips 1 mm thick and 0.25–0.3 g in fresh weight (FW) were cut from 15-mm long cylindrical sections of the unbarked branches. Control chips were placed in glass beakers and autoclaved at 121 °C for 15 min to inactivate intrinsic plant peroxidases (PO, EC 1.11.1.7) and vital-cell responses.

2.2. Oxidation of ABTS in the Presence of Sapwood Chips

Triplicate plastic cuvettes (1 cm) were used to incubate 1–2 live sapwood chips in 0.6 mL each of ABTS (6.6 mg/10 mL; Fluka); 0.1 M KH₂PO₄ buffer pH 4.5; and H₂O₂ 30% (15 mg/10 mL) prepared with bideionized water. Color reactions extending over 5 min to several h were followed at A₄₃₀; A₅₂₁; and A₅₅₀ as well as by scanning spectrophotometry (Helios Beta, Unicam UV-VIS, Cambridge, UK) after centrifugation of the supernatants at 14,000 g for 5 min. In the respective reference samples, H₂O₂ solution was replaced by water. The test arrangement was also used to incubate live sapwood chips with 0.1 mL of the laccase solution from a late liquid idiophase culture of the basidiomycete *Kuehneromyces mutabilis* grown in 25 g malt extract (Merck) and 5 g casein peptone L⁻¹ whereby H₂O₂ solution was replaced by water. Laccase solution was applied, too, upon incubations of autoclaved sapwood chips with inactivated PO, of mature wheat straw, and of green stem sections of the grass *Boa* spp. Several reactions were re-examined with commercial *Pyricularia oryzae* laccase (Sigma).

2.3. Molecular Size Separation of the ABTS Derivative by Ultrafiltration

A reaction mixture as above was incubated with sapwood chips of European beech at 22 °C for 8 h, using the constitutive plant peroxidase as the catalyst. The red oxidation product was centrifuged at 14,000 g for 10 min and scanned in the wavelength range of 340–800 nm. A 25-mL aliquot of the solution was transferred to a Centriscart 13239 filter (Sartorius, Germany) with a molecular size cutoff of 10 kDa and centrifuged at 2000 g. Subsequently, scans were taken from both the bright-red filtrate and the remaining dark-red concentrate fractions.

2.4. Extraction of Peroxidase from the Outer Sapwood

Samples of 0.5 g in dry weight (DW) were rasped from vital and unbarked branches Ø 12–20 mm and submerged in 5 mL of 0.2 M KH₂PO₄ buffer pH 4.5 at 6 °C for 4 h. Aliquots of the extracts were then transferred to 2-mL microtubes and stored at 6 °C. The peroxidase activity was determined by adding 0.1 mL of the centrifuged extract to 0.45 mL each of ABTS (6.6 mg/10 mL) and H₂O₂ 30% (15 mg/10 mL) solution prepared with 0.1 M KH₂PO₄ buffer pH 4.5. The production of the green ABTS^{•+} cation radical to be expressed in µM min⁻¹ was followed at A₄₂₀ for 12 min ($\epsilon_{420} = 36,000 \text{ M}^{-1} \text{ cm}^{-1}$) [57].

2.5. Extraction of Total Phenol from the Outer Sapwood

In quadruplicate test tubes, rasped outer sapwood samples 0.5 g in DW from vital branches of trees were suspended in 7 mL of bideionized water. Two samples were stored at 12 °C for 20 h before the aqueous extract was collected and centrifuged at 14,000 g for 5 min. The remaining two samples were boiled in a water bath at 98 °C for 1 h, compensated for weight losses with bideionized water, and stored up to 20 h at 12 °C.

A freshly prepared test solution of Fast Blue B Salt (O-dianisidine tetrazotized zinc chloride double salt; Acros) in 0.1 M KH₂PO₄ buffer pH 4.5 (10 mg mL⁻¹) was used as phenol reagent. Concentration values were spectrophotometrically determined. For a reaction mixture of 1 mL sapwood extract and 0.9 mL buffer, the initial A₅₀₀ value was recorded. After adding 0.1 mL of the phenol reagent, the spontaneous rise in the A₅₀₀ value was exactly read at 15 s. The test was repeated two times. From the increment in A₅₀₀, the absorbance value of 0.1 mL reagent in 1.9 mL buffer, reduced by the value of the buffer in the glass cuvette, was subtracted. Total phenol concentrations expressed as pyrogallol equivalents were calculated via calibration curve.

2.6. Solvent Extraction of Potential Redox Mediator Substances from Sapwood of European Beech

The extraction of rasped beech sapwood samples (0.5 g DW) with 5-mL aliquots of bideionized water, 80% methanol, and 80% acetone, respectively, followed the protocol used for total phenol extraction. Aliquots of the extracts obtained at 12 °C were transferred to 2-mL test tubes after 20 h of incubation and stored at 2 °C. Alternative water, methanol, and acetone treated samples were boiled in a water bath at 98 °C for 60, 30, and 10 min, respectively, compensated for the losses in solvent, and left standing for up to 20 h at 12 °C. The extracts were tested for the presence of redox mediators in ABTS oxidation assays. Apart from the cold-water extract with its plant PO constituents, the reaction mixtures of the organic solvent and hot solvent extracts had to be amended with *K.-mutabilis* laccase.

2.7. Examination of ABTS Derivative by Liquid Chromatography

A non-purified sample of ABTS derivative generated with the low-MW root exudates of white mustard (*Sinapis alba* L.) was analyzed by Liquid Chromatography with MS detection (LC-MS) and pneumatically assisted Atmospheric Pressure Ionization (API). The Perkin Elmer Sciex API 16 S with Series 200 pump and autosampler was run with 5.2 KV ionization voltage, 5 µL sample injection, and a flow of 0.25 mL min⁻¹ under isocratic conditions. The eluent was composed of 10% methanol, 85% AFFA A, and 5% AFFA B.

AFFA A: 50 mM formic acid, 2 mM NH₄⁺HCOO⁻ in water.

AFFA B: 50 mM formic acid, 2 mM NH₄⁺HCOO⁻ in 95% acetonitrile.

2.8. Oxidation of ABTS by Potassium Peroxodisulfate (K₂O₈S₂)

A reaction mixture of ABTS (190 mg L⁻¹; Fluka, > 99% HPLC grade; M 548.68) and K₂O₈S₂ (1.4 g L⁻¹; Merck, p. a. quality; M 270.33; molar ratio 1:15) prepared with bideionized water was incubated in duplicate 1-cm glass cuvettes at 20 °C. The color changes from green (ABTS^{•+}) and brownish black to the final deep lilac within 3 min to 96 h were followed by scanning spectrophotometry in the range of λ = 340–800 nm. The K₂O₈S₂ solution (1.4 g L⁻¹) served as reference sample and did not show any peaks in the 400–800 nm range. Bulk samples of the deep lilac and insoluble ABTS oxidation product were prepared in 2-mL microtubes by dissolving 2–3 mg ABTS and 20 mg K₂O₈S₂ in 1.5–2 mL of bideionized water (pH 2.37). Following reaction times of 3–5 min, the product could be separated from the colorless supernatant by centrifugation at 14,000 g for 5 min. The resulting pellet was cleaned from K₂O₈S₂ traces down to 2 × 10⁻⁶ and a final pH 3.5 by up to eight consecutive resuspensions and centrifugations in 1.8 mL batches of bideionized water.

2.9. Oxidative Discoloration of Remazol Brilliant Blue R (RBBR; M 626.5)

Stock solutions were prepared in 0.1 M KH₂PO₄ buffer pH 4.5 for RBBR at 2.1 mg/10 mL; for ABTS at 6.6 mg/10 mL; and for H₂O₂ 30% at 5 mg/10 mL. The red ABTS derivative was obtained from incubations with sapwood chips of beech and corresponded with a maximum of 0.22 mg mL⁻¹ of ABTS as the start substance. Combinations of the reaction mixtures are specified in Section 3. All incubations were performed at 22 °C.

2.10. Data Processing

In the case of numerical data, SPSS 8.0 software (Chicago, IL, USA) was used to calculate standard deviations (SD) of duplicate to quadruplicate results, linear correlations, and to perform one-way analyses of variance. To determine the positions of the comparatively flat peaks obtained by spectrophotometric scans of ABTS solutions in the A₃₄₀ to A₈₀₀ nm range, absorbance values of the curves were determined for 2-nm intervals. Peaks were accepted where the differences between neighboring intervals dropped to zero.

3. Results

3.1. Formation of ABTS Derivatives

The oxidation of ABTS by plant PO of beech did not terminate with the formation of the green-colored cation radical (ABTS^{•+}) if the live sapwood chip as the enzyme source was part of the reaction mixture. With the further oxidation to the ABTS derivative, the green color of the solution turned red within 1–8 h at room temperature. The product was stable and remained soluble by exposure to HCl and NaOH in the pH 0.5–14 range. Spontaneous reductions to the green ABTS^{•+} oxidation state upon applications of ABTS and the expected electron exchange by comproportionation [29] were not observed. The production of the ABTS derivative went along with the replacement of the peaks at A₄₂₀, A₆₄₅, and A₇₂₈, which are ascribed to the electrochemically generated ABTS^{•+} (Figure 2) [41], by rather flat ones in the A₅₂₀ to A₅₅₀ range. Both the wavelength positions and the total absorbance values of the peaks changed with species and accession of the timber, with the kind of the oxidoreductase enzyme involved (Table 1; Figure 2) and with the activation, e.g., of the intrinsic PO by variable doses of H₂O₂ (Figure 3). No further peaks followed those displayed in the 400–600 nm scans.

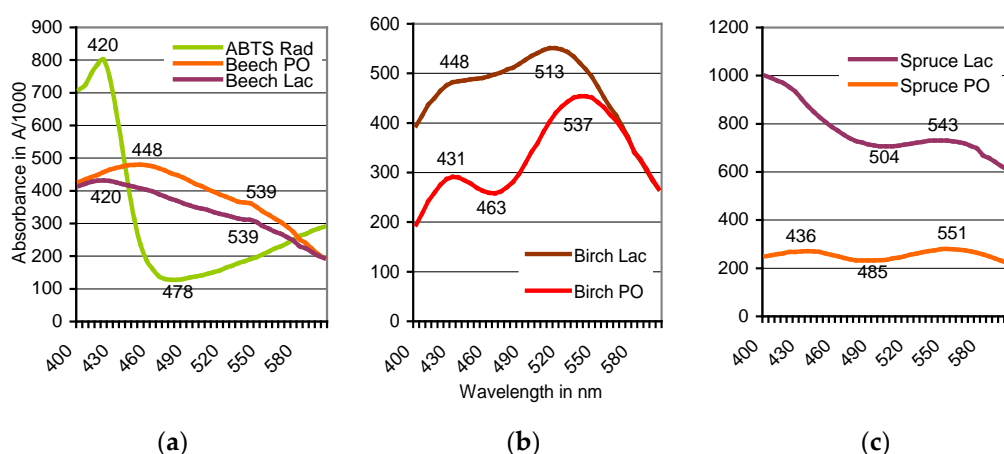


Figure 2. Oxidation of ABTS by sapwood internal peroxidase (PO)/external H₂O₂ systems and mushroom laccase (Lac), respectively, aided by redox mediators of beech (a), birch (b), and spruce (c). Scans A₄₀₀ to A₆₀₀ obtained for oak, sycamore, and pine the widest corresponded with those of beech, birch, and spruce, respectively. See Table 1 for positions of their absorbance peaks.

Table 1. Positions of absorbance peaks of the ABTS derivative in different wood species from February, 2014 as influenced by total phenol content and the enzyme catalyst.

Tree Species	Total Phenol ^a		Peak Absorbance (A) ^b	
	12 °C Extract	98 °C Extract	Peroxidase	Laccase
European beech	3309 ± 1107	9912 ± 653	A ₅₃₉ = 0.356	A ₅₃₉ = 0.312
Sycamore	180 ± 20	91 ± 0	A ₅₆₀ = 0.284	A ₅₆₆ = 0.190
European birch	98 ± 6	352 ± 7	A ₅₃₇ = 0.455	A ₅₁₃ = 0.551
Common oak	3227 ± 958	1915 ± 737	A ₅₄₂ = 0.190	A ₅₄₅ = 0.440
Hornbeam	231 ± 22	224 ± 4	No peak	No peak
Norway spruce	53 ± 3	66 ± 12	A ₅₅₁ = 0.280	A ₅₄₃ = 0.732
Scots pine	116 ± 32	64 ± 2	A ₅₆₀ = 0.329	A ₅₅₉ = 0.330

^a Total phenol given as pyrogallol equivalent in mg kg⁻¹ of dry wood extracted at 12 and 98 °C, respectively.

^b Active enzyme catalysts: sapwood peroxidase, activated by H₂O₂ supplements; laccase of *K. mutabilis*. The absorbance values corresponded with 0.22 mg mL⁻¹ ABTS in the original reaction mixture.

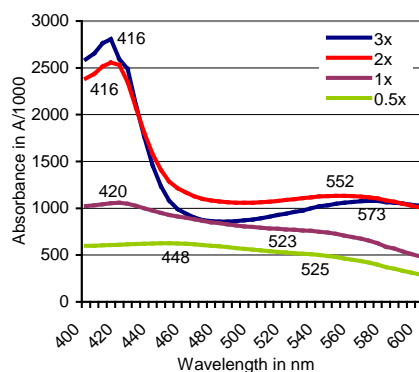


Figure 3. Doses of H_2O_2 rising in the range of 0.5–3 \times alter the positions of absorbance peaks of the ABTS derivative catalyzed by beech sapwood. In comparable tests with birch sapwood, the final peak moved with the rising H_2O_2 doses from A_{537} to A_{548} . Dose “1 \times ” refers to the H_2O_2 concentration given in Section 2.2.

Across the wood species, the reaction mixtures showed yellowish (hornbeam), red to red-brown (beech, oak), ruby (birch), and brown (spruce, pine) color tones. These may be influenced by concentration and composition of the easily extractable wood constituents, many of which may be phenolic in nature (Table 1) to yield colored compounds upon peroxidase and laccase catalyzed co-oxidations or polymerizations. The inherent peroxidase activities of the sapwood samples collected from January to June 2014 generally peaked in April, were higher in sapwood from understory rather than from dominant tree sources, and failed to correlate with the A_{550} values ($r = 0.033\text{--}0.364$). Similarly, the drastic drop to 3–5% in the total sapwood phenol content between February and June did not interfere with the formation rate of the ABTS derivative (data not specified).

The red ABTS derivative was formed both with the live PO bearing sapwood and the heat-treated one whose inactivated enzyme was compensated by commercial horseradish peroxidase or mushroom laccase supplements. Beech sapwood extracts drawn with water, methanol, and acetone at 12 or 98 °C were also able to replace the wood chip in the laccase supported catalysis of the ABTS derivative as they all contained the respective redox mediators. As shown in HPLC-MS assays, the compounds ranged 60 to 1400 in MW and reached from catechin and tryptophan to flavonoids (data not shown).

Incubation for 20–27 h at room temperature of 0.15 g mature wheat straw or of 0.2 g of the green stem tissue of *Boa* sp. in the ABTS/ KH_2PO_4 reaction mixtures amended with fungal laccase solution resulted, too, in the formation of the red ABTS derivatives in the absence of external H_2O_2 . The stable products showed single peaks at $A_{550}\text{--}A_{555}$ (straw) and $A_{527}\text{--}A_{531}$ (grass), respectively. Their handling in (possibly electrostatically loaded) vessels resulted sometimes in the transient appearance of $\text{ABTS}^{\bullet+}$ linked peaks at A_{430} and A_{728} . This was combined with shifts of the derivative peaks by 10–30 nm to higher values. In the presence of beech timber pre-degraded by soft rot and amended with laccase, the formation of the ABTS derivative was delayed for 3–4 days. Moreover, the soft-rotten timber samples generated the red derivative even in the absence of laccase (and H_2O_2) amendments within 7–9 d from ABTS solution. To the utmost surprise, in the presence of the non-purified fungal laccase, a reaction mixture composed of ABTS/ KH_2PO_4 without external H_2O_2 , that normally persists in the green $\text{ABTS}^{\bullet+}$ state, was also found converted to the red ABTS derivative with a peak at $A_{533}\text{--}A_{535}$ after 9 d in all replicates.

3.2. Transformation of $\text{ABTS}^{\bullet+}$ to the ABTS Derivative in the Absence of Oxidoreductases

Amending the ABTS/ KH_2PO_4 solution with fungal laccase yielded the stable $\text{ABTS}^{\bullet+}$ state at $A_{420} > 4.0$. The absorbance fell to 2.6–2.8 by boiling the solution in a water bath at 98 °C for 5 min to inactivate the laccase. Adding sapwood chips of beech whose enzyme had been inactivated by autoclaving resulted in the spontaneous abiotic-radical conversion of $\text{ABTS}^{\bullet+}$ to the red ABTS

derivative within 6–8 s and the reduction of a portion of the cation radical to the initial ABTS. The red derivative displayed a pronounced absorbance peak of $A_{535} = 0.174$ at $\lambda = 535\text{--}545$ nm (scan not shown). Reoxidizing the portion of the reduced ABTS with subsequent laccase applications increased the final absorbance values to $A_{535} = 0.42\text{--}0.45$.

3.3. Filtration of the Red ABTS Derivative Against a 10-kDa Cutoff

Filtration was terminated when the composite ABTS derivative (2.5 mL) produced with sapwood chips of beech had yielded a bright-red filtrate (molecular size ≤ 10 kDa) and a dark-red to brownish concentrate fraction (molecular size ≥ 10 kDa) in proportions of 73:27% (v/v; Figure 4). The derivative linked absorbance peak of the original composite fraction located at A_{520} moved to A_{515} in the filtrate and was lacking in the concentrate (Figure 5). Whereas applications of ABTS to both fractions did not result in spontaneous disproportionation reactions, adding H_2O_2 provoked the immediate greening in the concentrate, and a hesitant greening in the filtrate fraction due to contamination of the latter with PO traces in the close filter system. The respective solutions regained their red color within 2–4 days at room temperature. Applying the $\text{O}_2^{\bullet-}$ releasing KO_2 crystals known to reduce $\text{ABTS}^{\bullet+}$ [58] destroyed the red substances within 24 h.



Figure 4. Centrisart filter system with a 10 kDa cutoff in two magnifications separating filtrate (top); and concentrate (bottom) of an ABTS derivative catalyzed by European beech sapwood.

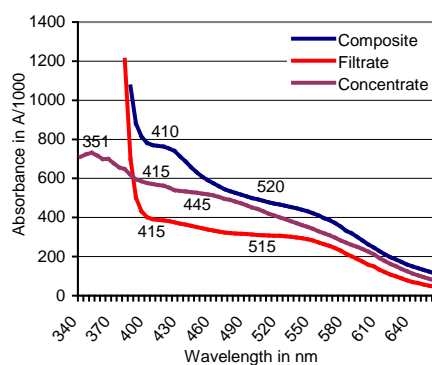


Figure 5. Filtration against a 10-kDa cutoff: Positions of absorbance peaks of the composite ABTS derivative as catalyzed by beech sapwood, of the filtrate ≤ 10 kDa, and the concentrate ≥ 10 kDa.

3.4. LC-MS Examination of a Non-Purified ABTS Derivative from White Mustard

Under the ionizing conditions of the weak acids in the eluent, the red ABTS derivative yielded major peaks at m/z 452.6 > 490.4 > 485.3. Among the numerous minor substances, m/z 514.1 to 514.2 represented the ABTS dianion molecule completed by two protons at the former NH_4 binding sites. A derivative appearing at m/z 486.3 points to additional demethylations that are replaced by two H^+ (Figure 6).

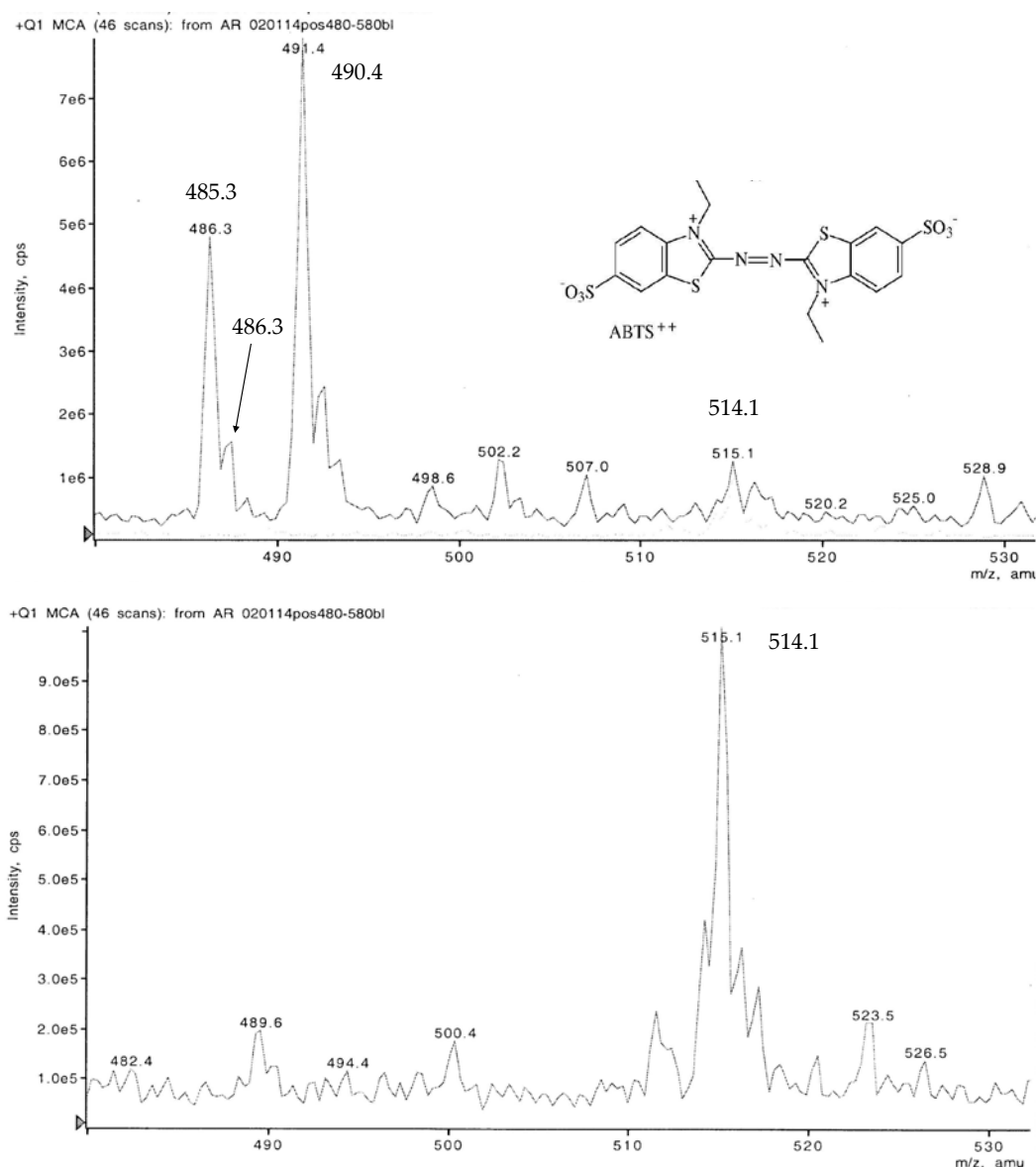


Figure 6. LC-MS chromatograms in the positive mode of a non-purified ABTS derivative with the protonated dianion of ABTS⁽²⁺⁾ (m/z 514.1), its deethylated (C₂H₅) form recompleted by methyl groups (CH₃, m/z 486.3), and major ABTS moieties.

3.5. Chemical ABTS Oxidation

Molarities of 1:2 between ABTS and K₂O₈S₂ in the reaction mixture completed the oxidation of the ABTS to the green cation radical with its slightly higher values shifted peaks at $\lambda = 420/660/738$ nm within 20–45 min. A black to blue-green color was observed at 4 h and did not show any further changes within 96 h. The green color spontaneously developed in dilute reaction mixtures with molarities of 1:15. Changes to brownish black and the disappearance of the A₄₂₂ peak accompanied the formation of the final deep lilac reaction product within 2 h (Figure 7). Diluted aliquots were reddish violet and contained clouds of precipitates which formed deep lilac pellets in the colorless supernatants of non-depleted K₂O₈S₂ solution of pH 2.15 upon centrifugation. Pellets obtained from bulk samples of 5 mg ABTS were separated from K₂O₈S₂ residues by up to 10 consecutive re-suspensions and centrifugations in 2-mL aliquots of bideionized water. The washing fluids increasing in pH from 2.7 to the stable 3.6 contained the green ABTS^{•+} at absorbance values of around A₄₂₀ = 0.8. This moderate release of ABTS^{•+} did not substantially increase in NaOH amended washing fluids of pH 8.0. In NaOH

solutions of pH 11, the precipitates were dissolved by the consecutive reduction to the green ABTS cation radical and the final colorless ABTS within 1 h. Dispersing the separated and rinsed precipitates in aqueous ABTS solution resulted in the spontaneous appearance of green at absorbance values of $A_{420} > 2.5$. Thus, the precipitates indicated their nature as active oxidants by comproportionation with ABTS.

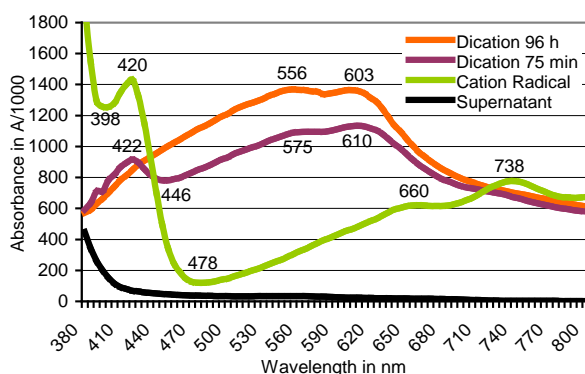
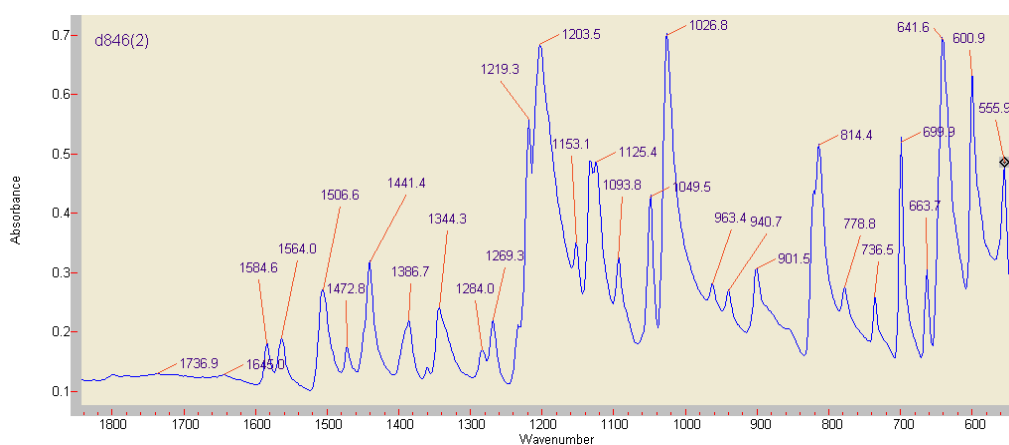


Figure 7. Oxidation of ABTS with potassium peroxodisulfate as followed by scanning spectrophotometry. The peaks at $\lambda = 420/660/738$ nm shown by the green ABTS^{•+} oxidation state (reaction time, 10 min) are replaced by peaks around 556/603 nm of the deep lilac and flocculent (insoluble) reaction product (reaction time, 75 min to 96 h) which precipitates in the colorless supernatant of non-depleted $K_2O_8S_2$ solution of pH 2.15.

3.6. Comparison of ABTS Derivatives by Fourier Transform Infrared Spectroscopy (FT-IR) Analyses

Differences in composition and stability of the red ABTS derivatives obtained by chemical or enzymatic oxidation were drastically illustrated by preliminary FT-IR analyses (Figure 8). The lilac precipitates of the completely by $K_2O_8S_2$ oxidized monoazo compound (formed from 3.7 mg ABTS) showed major stretching vibrations at 1506.6, 1472.8, and 1441.4 cm^{-1} , i.e., in the range of (1555) 1525–1410 cm^{-1} associated with the presence of the $-N=N-$ double bonds in the majority of azo dyes [59–62]. The compound generated by fresh beech wood chips (compare Section 2.2; 1.7 mg ABTS in 40 mg KH_2PO_4) showed then the azo group related band at 1473.77 cm^{-1} in an environment of a general structural decay, with the dominance of signals from P-O bonds around 859 cm^{-1} (Figure 8) [63].



(a)

Figure 8. Cont.

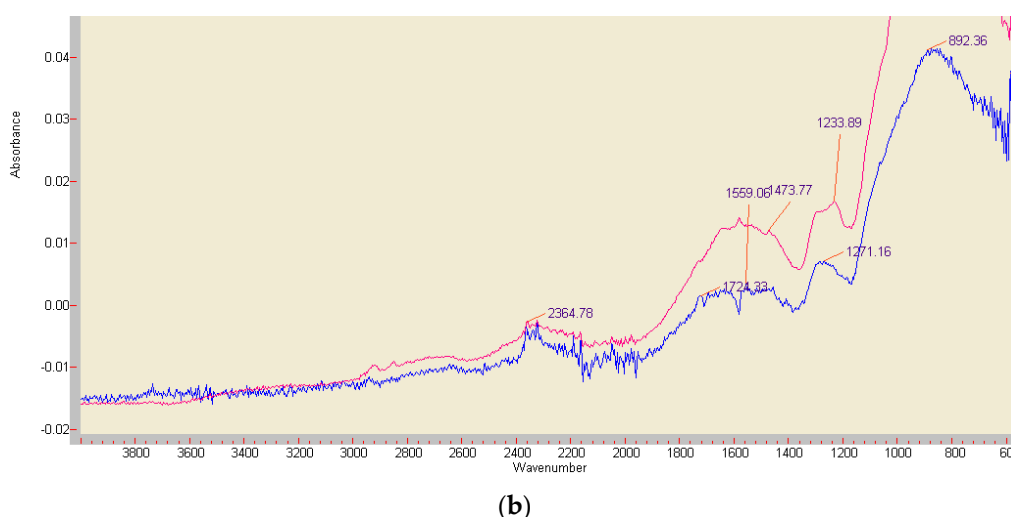


Figure 8. FT-IR analyses of the red ABTS derivatives obtained by $K_2O_8S_2$ oxidation (a), and of the product generated by enzymatically active beech wood chips (b) (red curve), paired with an ABTS-free reference sample (blue curve). The major peak at 858.86 cm^{-1} is not shown.

3.7. Discoloration of Remazol Brilliant Blue R

In two test arrangements, the promoting effect of the red ABTS derivative on the oxidative discoloration of the dye RBBR was significant ($p \leq 0.01$). In the Table 2 test, applications of *K. mutabilis* culture fluid solely exposed the RBBR solution to the fungal laccase activity. Adding H_2O_2 as an enzyme co-substrate activated the oxidative cycle of the fungal MnP in the narrow frame set by the presence of free Mn cations, whereas an equivalent of 0.044 mg ABTS was applied with the input of 0.2 mL of the red ABTS derivative generated with beech sapwood. The resulting absorbance values A_{595} for RBBR dropped in proportions of 1 (Lac):1.3 (Lac; MnP):3.3 (Lac; MnP; ABTS derivative). Additional applications of ABTS gave rise to the formation of the stable green $ABTS^{\bullet+}$ solution which masked any effects on the discoloration of RBBR.

Table 2. Discoloration of Remazol Brilliant Blue R in duplicate plastic cuvettes within the first ten min of reaction. Enzyme, culture fluid of *K. mutabilis* with laccase and MnP activity.

Composition of the Reaction Mixture (mL) ^a	Active Oxidants	$A_{595}\text{ Loss min}^{-1} (\pm SD)$
RBBR, 0.5; buffer, 0.5; enzyme, 0.1	Lac	0.0147 ± 0.0021
RBBR, 0.5; buffer, 0.3; H_2O_2 , 0.2; enzyme, 0.1	Lac; MnP	0.0193 ± 0.0018
RBBR, 0.5; buffer, 0.1; H_2O_2 , 0.2; enzyme, 0.1; ABTS derivative, 0.2	Lac; MnP; ABTS derivative	0.0486 ± 0.0037

^a See Section 2.2 for details.

The tests shown in Table 3 with sapwood chips of beech used the plant PO/ H_2O_2 couple in concert with its natural mediators as the catalytic system. Relative to this control, the absorbance values A_{595} decreased significantly with the application of ABTS and ABTS/ABTS derivative ($p \leq 0.05$), respectively, in proportions of 1 (PO):1.14 (PO; ABTS):1.83 (PO; ABTS; ABTS derivative). The presence of the widest sapwood chips prevented the dominance of a green $ABTS^{\bullet+}$ component in the reaction mixture.

Table 3. Discoloration of RBBR in duplicate 1-cm plastic cuvettes catalyzed by the peroxidase of two sapwood chips each of European beech.

Composition of the Reaction Mixture (mL) ^a	Active Oxidants	A ₅₉₅ Loss min ⁻¹ (±SD) after	
		5 h	50 h
RBRR, 1; H ₂ O ₂ , 0.5; buffer, 0.2	PO	0.231 ± 0.016	0.569 ± 0.038
RBRR, 1; H ₂ O ₂ , 0.5; ABTS, 0.2	PO; ABTS derivative	0.264 ± 0.024	0.638 ± 0.044
RBRR, 1; H ₂ O ₂ , 0.5; ABTS, 0.1; ABTS derivative, 0.1	PO; ABTS derivative	0.422 ± 0.036	0.704 ± 0.032

^a See Section 2.2 for details.

4. Discussion

The transformation of the green ABTS^{•+} solution to stable reddish products in the presence of lignocelluloses such as fresh and rotten timber, straw, and green herbage is possibly a hitherto non-reported phenomenon. The absorbance peaks of the transformation products appear at wavelength positions within $\lambda = 513\text{--}573$ nm and exceed the narrow span of 518–520 nm reported for the electrochemically [30,41] and wet-chemically [44,45] generated ABTS²⁺. Testing several inorganic peroxides yielded a further ABTS oxidation product that showed absorbance peaks at around A₄₂₀ and A₅₃₀ in scans [45] that resemble those given for the red ABTS derivatives in the Figures 3 and 5. The authors failed to purify the respective products and took them for sulfoxide and sulfone compounds obtained from ABTS^{•+} and the oxidants peroxomonosulfate and peroxodiphosphate. Majcherczyk et al. [46] obtained “a small amount of a reddish product” absorbing at $\lambda = 560\text{--}570$ nm upon the oxidation of veratryl alcohol with laccase/ABTS. A similar red product appearing at 562 nm was obtained from ABTS^{•+} in the presence of bovine serum albumin but also in Mes buffer solvent [64]. During repeated recoveries and re-oxidations with acetone and laccase, respectively, a purple by-product deduced to be azodication was gradually formed. Filtration against a 10 kDa cutoff separated a colorless filtrate from magenta colored substances the authors took for ABTS²⁺-laccase complexes [65].

The present tests with vital sapwood chips from seven European tree species show that color, wavelength position and total absorbance of the ABTS^{•+} transformation products vary with timber species and their accession, with the kind of the enzyme catalyst, and the amount of the applied H₂O₂ as the exhaustible activator of the wood-intrinsic peroxidases (Table 1, Figures 2 and 3). Co-oxidations and polymerizations of specific timber extractives as well as complex and adduct formations may then account for shifts of the absorbance peaks within the visible light spectrum.

Whereas the formation of the ABTS cation radical in the laccase-ABTS mediator system is enzyme catalyzed, its transformation to the reddish product is a spontaneous abiotic reaction with mediating extractives of lignocelluloses. Applying autoclaved beech sapwood chips with their heat-inactivated peroxidase to boiled ABTS^{•+} solution resulted in the formation of red products and the reduction of the remaining cation radical within 6–8 s in the absence of enzymes (Section 3.2). The reduction of ABTS^{•+} to ABTS comprises the one-electron oxidation of the lignocellulose extractives to radicals that overcome the potential of $E^0 = 1.09$ V during the formation of the azodication from ABTS^{•+}, with the promise to play a major part in the initial attacks on plant lignins, too. The respective extractives drawn with water or organic solvents from beech sapwood mimicked the mediating catalytic effect of the live and heat-killed timber and comprised molecules ranging 60 to 1400 in MW as shown by HPLC-MS analyses. Related extractives determined for wheat straw were N-heterocycles (16–29%), fatty acids (19–26%), and phenols (12–23%) beside carbohydrates, amino acids, n-alkyl benzenes, diols, sterols, steroids, and flavonoids in the m/z range 270–414 [66]. In the case of phenolics, redox mediating effects have long been known. Phenol, cresol and resorcinol enabled plant peroxidase to form the abiotic oxidant Mn³⁺ [67]. Common phenolics with redox potentials E^0 between 0.54–1.23 V [14,19,32,34] but also the metabolite 3-hydroxyanthranilate of the wood-decay fungus *Pycnoporus cinnabarinus* [11] showed potential as laccase mediators.

Ultrafiltration against a 10 kDa cutoff separated a beech wood catalyzed red transformation product peaking at $\lambda = 520$ nm into a bright-red filtrate (peak at A_{515}) and a darker red concentrate without the typical ABTS derivative related peak (Figures 4 and 5). ABTS application to the filtrate (and the concentrate) did not result in a spontaneous comproportionation [41,46] of the red substance(s) although handling of comparable products from green herbage in presumably electrostatically loaded vessels gave rise to a transient re-appearance of $ABTS^{\bullet+}$ related peaks in spectrophotometric scans. The respective peaks disappeared again by the non-enzymatic transformation of $ABTS^{\bullet+}$ to the red derivative in the presence of (less efficient or lower concentrated?) lignocellulose extractives from grasses. In the concentrate fraction, application of ABTS plus H_2O_2 led to the immediate formation of $ABTS^{\bullet+}$ by the enriched peroxidase constituents of 31.9–39.4 kDa in MW [55]. This was followed again by the formation of red products. The darker red tone of the concentrate compared to the filtrate fraction suggests a relative enrichment of the red derivatives (bound in complexes?) with high-MW compounds and especially an adduct constellation with (enzyme) proteins [30,65,68,69].

Liquid chromatograms of a non-purified red ABTS derivative generated by white mustard root exudates showed a peak at m/z 514.2 (Figure 6). This corresponds with all oxidation states of ABTS M 548.68 deprived of both NH_4 moieties (Figure 1) and re-complexed by two (H^+) protons. A peak at m/z 486.3 points to the replacement of both ethyl (C_2H_5) by methyl (CH_3) groups of this compound. The main peaks appeared at m/z 490.4, 485.3, and 452.6. The substances should be ABTS derived but also linked with substrate components as they surpass by far the concentrations and the low-MW range of the carbohydrate and aliphatic and aromatic acid traces exuded by white mustard seedlings in axenic culture [70,71]. In comparable HPLC-MS assays, the radical content of vegetable extracts is determined by the quantitative discoloration (reduction) of a green $ABTS^{\bullet+}$ solution. Beside the m/z 514 peak valid for all protonated ABTS dianion moieties as above, the MS protocols show, e.g., adduct formations between $ABTS^{2+}$ and the radical scavenging flavonols rutin, hyperoside, quercetin, and quercitrin compounds [72]. The FT-IR analysis of the enzymatically generated ABTS derivative indicated, beside the wide destruction of the molecule, conserved structures in the chromogenic environment of the $-N=N-$ double bond. Its position at 1473.77 cm^{-1} corresponds with the vibration stretch at 1472.8 cm^{-1} of the $K_2O_8S_2$ oxidized product (Figure 8). Nevertheless, in the case of the chemically identical structures of $ABTS^{\bullet+}$ at pH 1.5 and an $ABTS^{2+}$ preparation in concentrated HNO_3 , Raman spectroscopy yielded different spectra [43].

The red multi-component and water-soluble ABTS derivative pretended stability from pH 0.5 (HCl) to pH 14 (NaOH) and was destroyed by $O_2^{\bullet-}$ released from KO_2 . In contrast, the $ABTS^{2+}$ product presented, e.g., by Majcherczyk et al. [46] and generated with potassium peroxodisulfate formed double peaks at $\lambda = 556$ and 603 nm (Figure 7), precipitated from a supernatant pH 2.15, and was reduced to ABTS by comproportionation and higher alkaline conditions (pH 11, NaOH). It oxidized several non-phenolic alcohols [46]. Elemental analyses of the washed precipitate by ICP-MS suggested that the insolubility of the product was not due to the binding of $K_2O_8S_2$ derived K^+ to the so far complete $ABTS^{2-}$ dianion (Figure 1) in the pH range of up to 3.5 (data not shown).

The catalytic potential of the red ABTS derivative needs further investigations. Its use in combination with the non-purified *K. mutabilis* laccase and with H_2O_2 accelerated the bleaching of the dye RBBR significantly (Table 2). Its bleaching was also stimulated when not only the live sapwood chip of beech with its natural mediators but also an amount of the red ABTS derivative was applied (Table 3) that, it should not be concealed, contained active radicals derived from timber extracts.

The results invite to a reappraisal of an old controversy (e.g., [29,30]): is the cell-free and purified laccase/ABTS couple able to form $ABTS^{2+}$ in vitro? According to Christensen and Kepp [68], the turnover of ABTS is optimal by laccases with positively charged anchor points in their pockets near the T1 copper site. This positive charge should correspond with ABTS at pH values > 3 (pK_a around 2) that appears as $ABTS^{2-}$ dianion deprived of both NH_4 moieties (Figure 1). At pH 4.5, the enzyme (E^0 up to 0.79 V) would oxidize around 50% of the ABTS pool [73,74] to the green $ABTS^{\bullet-}$ radical anion ($E^0 = 0.68$ V) [41] by one-electron abstraction. If the enzyme catalyzed accidental oxidations of

the radical to dications in a numerical redox reaction it cannot afford ($E^0 = 1.09$ V) [41], the dications would comproportionate with ABTS back to the radical state. Indirect evidence for $ABTS^{2+}$ formations by laccase/ABTS is being derived from reactions of the couple with high redox potential substrates such as veratryl alcohol (3,4-dimethoxybenzyl alcohol) ($E^0 = 1.4$ V) and other benzyl alcohols that are frequently tested in the citrate and acetate buffers used by Cyclic Voltammetry [29,30,46,52,53]. The respective substrates could be contaminated by organic traces with mediator properties similar to those of wood extractives.

Amending an enzyme generated and subsequently boiled $ABTS^{\bullet+}$ solution with autoclaved beech wood caused its partial transformation to the red ABTS derivative within 6–8 s in an abiotic reaction with wood extractives and in the absence of functional enzymes (Section 3.2). The tests run over 1–2 h were repeated several times. This time span should not suffice that the red ABTS derivative had been formed with the aid of substrate contaminants as long as the enzyme had been active. Therefore, reactions of the laccase/ $ABTS^{\bullet+}$ couple that suggest catalytic contributions of $ABTS^{2+}$ should be reconsidered. Organic trace contaminants of test substrate, redox mediator, buffer, and the enzyme itself could initiate the abiotic $ABTS^{\bullet+}$ to $ABTS^{2+}$ conversion by acting like wood extractives, with the dication generating further radicals from substrates and their contaminants in the *stadium nascenti*. Further dications may immediately be trapped and stabilized as “slowly generated red substances” [45,46,64]. The transformation of an $ABTS^{\bullet+}/KH_2PO_4$ solution to the red ABTS derivative by mushroom laccase added as part of a depleted and multi-contaminant malt/peptone nutrient solution as late as after 9 days may serve as a precedent. Bourbonnais et al. [29] recorded ABTS mediated lignin oxidation at the redox potential of laccase (585 mV) at a very slow rate. The oxidation of 2,4-dimethoxybenzyl alcohol by laccase/ABTS started first with the onset of a second and slower rate of oxygen consume the authors linked with the slow production of $ABTS^{2+}$ in the initially formed laccase/ $ABTS^{\bullet+}$ solution [52]. Interactions of oxidoreductase enzyme/ABTS couples with the extractives of lignocelluloses drive these reactions to the utmost. In summary, it is uncontested that ABTS improves the efficacy of substrate conversions by oxidoreductases, irrespective of its presence as a transitory dication or a (red) multicomponent derivative.

5. Conclusions

There are no reasons to contest the importance of the ABTS dication in expanding the substrate ranges of laccases and plant peroxidases to higher-redox-potential substrates in vitro. Nevertheless, in the presence of lignocelluloses that contain a plethora of lower-MW extractives, the further conversion of the enzyme-catalyzed ABTS cation radical is a spontaneous and abiotic process that is complete within seconds. Its outcome may be the formation of radicals from lower-redox-potential extractives in a chain reaction initiated by $ABTS^{\bullet+}$ upon its reduction to functional ABTS, the apparent formation of a red ABTS derivative that possibly contains a stable form of $ABTS^{2+}$ beside high-MW adducts, and further ABTS moieties of MW > 400 Da, catalyzed by radicals derived from extractives or formed as artifacts under LC-MS conditions. Whether these ABTS moieties contribute more to oxidative degradation processes than the apparently to radicals transformed lignocellulose extractives is subject to further studies which may be rendered more difficult by the use of chemicals certified as “pure”.

Acknowledgments: The author is obliged to Dr. Volker Schulz, JenaBios GmbH Jena, Germany, for conducting FT-IR analyses; to Dr. Michael Reichelt, Max-Planck-Institute of Chemical Ecology, Department of Biochemistry, in Jena, Germany, for analyzing beech wood extractives by HPLC-MS; and to Dipl.-Chemist Klaus-Dieter Voigt, Food Analytics and Consulting, Jena, for conducting ICP-MS analyses of $ABTS/K_2O_8S_2$ constellations.

Conflicts of Interest: The author declares no conflict of interest.

References

1. Schachtschabel, P.; Blume, H.P.; Brümmer, G.; Hartge, K.H.; Schwertmann, U. *Lehrbuch der Bodenkunde*, 14th ed.; Enke: Stuttgart, Germany, 1998.
2. Fengel, D.; Wegener, G. *Wood: Chemistry, Ultrastructure, Reactions*; De Gruyter: Berlin, Germany, 1984.

3. Ballesteros, I.; Negro, M.J.; Oliva, J.M.; Cabañas, A.; Manzanares, P.; Ballesteros, M. Ethanol production from steam-explosion pretreated wheat straw. *Appl. Biochem. Biotechnol.* **2006**, *129–132*, 496–508. [[CrossRef](#)]
4. Han, L.; Feng, J.; Zhang, S.; Ma, Z.; Wang, Y.; Zhang, X. Alkali pretreated of wheat straw and its enzymatic hydrolysis. *Braz. J. Microbiol.* **2012**, *43*, 53–61. [[CrossRef](#)] [[PubMed](#)]
5. Khan, T.S.; Mubeen, U. Wheat straw: A pragmatic overview. *Curr. Res. J. Biol. Sci.* **2012**, *4*, 673–675.
6. Brodeur, G.; Yau, E.; Badal, K.; Collier, J.; Ramachandran, K.B.; Ramakrishnan, S. Chemical and physicochemical pretreatment of lignocellulosic biomass: A review. *Enzyme Res.* **2011**. [[CrossRef](#)] [[PubMed](#)]
7. Kristensen, J.B.; Thygesen, L.G.; Felby, C.; Jørgensen, H.; Elder, T. Cell-wall structural changes in wheat straw pretreated for bioethanol production. *Biotechnol. Biofuels* **2008**, *1*, 5. [[CrossRef](#)] [[PubMed](#)]
8. Arora, D.S.; Sharma, R.K. Ligninolytic fungal laccases and their biotechnological applications. *Appl. Biochem. Biotechnol.* **2010**, *160*, 1760–1788. [[CrossRef](#)] [[PubMed](#)]
9. Kirk, T.K.; Farrell, R.L. Enzymatic “combustion”: The microbial degradation of lignin. *Annu. Rev. Microbiol.* **1987**, *41*, 465–505. [[CrossRef](#)] [[PubMed](#)]
10. Wang, L.; Nie, Y.; Tang, Y.-Q.; Song, X.-M.; Cao, K.; Sun, L.-Z.; Wang, Z.-J.; Wu, X.-L. Diverse bacteria with lignin degrading potentials isolated from two ranks of coal. *Front. Microbiol.* **2016**, *7*, 1428. [[CrossRef](#)] [[PubMed](#)]
11. Eggert, C.; Temp, U.; Dean, J.F.D.; Eriksson, K.-E.L. A fungal metabolite mediates degradation of non-phenolic lignin structures and synthetic lignin by laccase. *FEBS Lett.* **1996**, *391*, 144–148. [[CrossRef](#)]
12. Gramss, G. Potential contributions of oxidoreductases from alfalfa plants to soil enzymology and biotechnology: A review. *J. Nat. Sci. Sustain. Technol.* **2012**, *6*, 169–223.
13. Husain, Q. Peroxidase mediated decolorization and remediation of wastewater containing industrial dyes: A review. *Rev. Environ. Sci. Biotechnol.* **2010**, *9*, 117–140. [[CrossRef](#)]
14. Johannes, C.; Majcherczyk, A. Natural mediators in the oxidation of polycyclic aromatic hydrocarbons by laccase mediator systems. *Appl. Environ. Microbiol.* **2000**, *66*, 524–528. [[CrossRef](#)] [[PubMed](#)]
15. Singh, G.; Kaur, K.; Puri, S.; Sharma, P. Critical factors affecting laccase-mediated biobleaching of pulp in paper industry. *Appl. Microbiol. Biotechnol.* **2015**, *99*, 155–164. [[CrossRef](#)] [[PubMed](#)]
16. Torres, C.E.; Negro, C.; Fuente, E.; Blanco, A. Enzymatic approaches in paper industry for pulp refining and biofilm control. *Appl. Microbiol. Biotechnol.* **2012**, *96*, 327–344. [[CrossRef](#)] [[PubMed](#)]
17. Kudanga, T.; Le Roes-Hill, M. Laccase applications in biofuels production: Current status and future prospects. *Appl. Microbiol. Biotechnol.* **2014**, *98*, 6525–6542. [[CrossRef](#)] [[PubMed](#)]
18. Parawira, W.; Tekere, M. Biotechnological strategies to overcome inhibitors in lignocellulose hydrolysates for ethanol production: Review. *Crit. Rev. Biotechnol.* **2011**, *31*, 20–31. [[CrossRef](#)] [[PubMed](#)]
19. Ayala, M.; Roman, R.; Vazquez-Duhalt, R. A catalytic approach to estimate the redox potential of heme-peroxidases. *Biochem. Biophys. Res. Commun.* **2007**, *357*, 804–808. [[CrossRef](#)] [[PubMed](#)]
20. Hofrichter, M.; Ullrich, R.; Pecyna, M.J.; Liers, C.; Lundell, T. New and classic families of secreted fungal heme peroxidases. *Appl. Microbiol. Biotechnol.* **2010**, *87*, 871–897. [[CrossRef](#)] [[PubMed](#)]
21. Wong, D.W.S. Structure and action mechanism of ligninolytic enzymes. *Appl. Biochem. Biotechnol.* **2009**, *157*, 174–209. [[CrossRef](#)] [[PubMed](#)]
22. Cui, F.; Dolphin, D. The role of manganese in model systems related to lignin biodegradation. *Holzforschung* **1990**, *44*, 279–283. [[CrossRef](#)]
23. Hammel, K.E.; Jensen, K.A., Jr.; Mozuch, M.D.; Landucci, L.L.; Tien, M.; Pease, E.A. Ligninolysis by a purified lignin peroxidase. *J. Biol. Chem.* **1993**, *268*, 12274–12281. [[PubMed](#)]
24. Nousiainen, P.; Kontro, J.; Manner, H.; Hatakka, A.; Sipila, J. Phenolic mediators enhance the manganese peroxidase catalyzed oxidation of recalcitrant lignin model compounds and synthetic lignin. *Fungal Genet. Biol.* **2014**, *72*, 137–149. [[CrossRef](#)] [[PubMed](#)]
25. Kersten, P.J.; Kalyanaraman, B.; Hammel, K.E.; Reinhammar, B. Comparison of lignin peroxidase, horseradish peroxidase and laccase in the oxidation of methoxybenzenes. *Biochem. J.* **1990**, *268*, 475–480. [[CrossRef](#)] [[PubMed](#)]
26. Kawai, S.; Umezawa, T.; Higuchi, T. Degradation mechanisms of phenolic β -1 lignin substructure model compounds by laccase of *Coriolus versicolor*. *Arch. Biochem. Biophys.* **1988**, *262*, 99–110. [[CrossRef](#)]
27. Kawai, S.; Umezawa, T.; Shimada, M.; Higuchi, T. Aromatic ring cleavage of 4,6-di(tert-butyl) guaiacol, a phenolic lignin model compound, by laccase of *Coriolus versicolor*. *FEBS Lett.* **1988**, *236*, 309–311. [[CrossRef](#)]

28. Bourbonnais, R.; Paice, M.G.; Freiermuth, B.; Bodie, E.; Borneman, S. Reactivities of various mediators and laccases with kraft pulp and lignin model compounds. *Appl. Environ. Microbiol.* **1997**, *63*, 4627–4632. [[PubMed](#)]
29. Bourbonnais, R.; Leech, D.; Paice, M.G. Electrochemical analysis of the interactions of laccase mediators with lignin model compounds. *Biochim. Biophys. Acta* **1998**, *1379*, 381–390. [[CrossRef](#)]
30. Branchi, B.; Galli, C.; Gentili, P. Kinetics of oxidation of benzyl alcohols by the dication and radical cation of ABTS. Comparison with laccase-ABTS oxidations: An apparent paradox. *Org. Biomol. Chem.* **2005**, *3*, 2604–2614. [[CrossRef](#)] [[PubMed](#)]
31. Brijwani, K.; Rigdon, A.; Vadlani, P.V. Fungal laccases: Production, function, and applications in food processing. *Enzyme Res.* **2010**. [[CrossRef](#)] [[PubMed](#)]
32. Camarero, S.; Ibarra, D.; Martínez, M.J.; Martínez, A. Lignin-derived compounds as efficient laccase mediators for decolorization of different types of recalcitrant dyes. *Appl. Environ. Microbiol.* **2005**, *71*, 1775–1784. [[CrossRef](#)] [[PubMed](#)]
33. Camarero, S.; Cañas, A.I.; Nousiainen, P.; Record, E.; Lomascolo, A.; Martínez, M.J.; Martínez, A.T. *p*-Hydroxycinnamic acids as natural mediators for laccase oxidation of recalcitrant compounds. *Environ. Sci. Technol.* **2008**, *42*, 6703–6709. [[CrossRef](#)] [[PubMed](#)]
34. Cañas, A.I.; Alcalde, M.; Plou, F.; Martínez, M.J.; Martínez, A.T.; Camarero, S. Transformation of polycyclic aromatic hydrocarbons by laccase is strongly enhanced by phenolic compounds present in soil. *Environ. Sci. Technol.* **2007**, *41*, 2964–2971. [[CrossRef](#)] [[PubMed](#)]
35. Díaz-González, M.; Vidal, T.; Tzanov, T. Phenolic compounds as enhancers in enzymatic and electrochemical oxidation of veratryl alcohol and lignins. *Appl. Microbiol. Biotechnol.* **2011**, *89*, 1693–1700. [[CrossRef](#)] [[PubMed](#)]
36. Gubernatorova, T.N.; Dolgonosov, B.M. Modeling the biodegradation of multicomponent organic matter in an aquatic environment: 3. Analysis of lignin degradation mechanisms. *Water Res.* **2010**, *37*, 332–346. [[CrossRef](#)]
37. Bourbonnais, R.; Paice, M.G.; Reid, I.D.; Lanthier, P.; Yaguchi, M. Lignin oxidation by laccase isozymes from *Trametes versicolor* and role of the mediator 2,2'-azinobis(3-ethylbenzothiazoline-6-sulfonate) in kraft lignin depolymerization. *Appl. Environ. Microbiol.* **1995**, *61*, 1876–1880. [[PubMed](#)]
38. Niladevi, K.N. Characterization of Laccase from *Streptomyces Psammoticus*: An Enzyme for Eco-Friendly Treatment of Environmental Pollutants. Ph.D. Thesis, Biotechnology Division, National Institute for Interdisciplinary Science and Technology (CSIR), Trivandrum 695 OI9, India, 2008.
39. Masoudian, S.; Rasoulifard, M.H.; Pakravan, P. Degradation of acid red 14 in contaminated water by Ag-SiO₂ nanocomposite. *Ind. J. Chem.* **2015**, *54*, 757–761.
40. Kim, S.Y. Synthesis, Characterization, and Applications of Conducting Polymers with Functional Dopants. Ph.D. Thesis, The School of Engineering and the Division of Biology and Medicine at Brown University, Providence, RI, USA, 2011.
41. Scott, S.L.; Chen, W.-J.; Jjakac, A.; Espenson, J.H. Spectroscopic parameters, electrode potentials, acid ionization constants, and electron exchange rates of the 2,2'-azinobis(3-ethylbenzothiazoline-6-sulfonate) radicals and ions. *J. Phys. Chem.* **1993**, *97*, 6710–6714. [[CrossRef](#)]
42. Bolis, C.; Huwig, A.K.; Grimm, R.; Rheinberger, V.M. Agents for Bleaching Teeth. U.S. Patent 20050158251, 21 July 2005.
43. Garcia-Leis, A.; Jancura, D.; Antalík, M.; Garcia-Ramos, J.V.; Sanchez-Cortes, S.; Jurasekova, Z. Catalytic effects of silver plasmonic nanoparticles on the redox reaction leading to ABTS•⁺ formation studied using UV-visible and Raman spectroscopy. *Phys. Chem. Chem. Phys.* **2016**, *18*, 26562–26571. [[CrossRef](#)] [[PubMed](#)]
44. Maruthamuthu, P.; Venkatasubramanian, L.; Dharmalingam, P. A fast kinetic study of formation and decay of 2,2'-azinobis(3-ethylbenzothiazoline-6-sulfonate) radical cation in aqueous solution. *Bull. Chem. Soc. Jpn.* **1987**, *60*, 1113–1117. [[CrossRef](#)]
45. Venkatasubramanian, L.; Maruthamuthu, P. Kinetics and mechanism of formation and decay of 2,2'-azinobis(3-ethylbenzothiazole-6-sulphonate) radical cation in aqueous solution by inorganic peroxides. *Int. J. Chem. Kinet.* **1989**, *21*, 399–421. [[CrossRef](#)]
46. Majcherczyk, A.; Johannes, C.; Hüttermann, A. Oxidation of aromatic alcohols by laccase from *Trametes versicolor* mediated by the 2,2'-azino-bis-(3-ethylbenzothiazoline-6-sulphonic acid) cation radical and dication. *Appl. Microbiol. Biotechnol.* **1999**, *51*, 267–276. [[CrossRef](#)]

47. Ley, C.; Zengin Çekiç, S.; Kochius, S.; Mangold, K.-M.; Schwaneberg, U.; Schrader, J.; Holtmann, D. An electrochemical microtiter plate for parallel spectroelectrochemical measurements. *Electrochim. Acta* **2013**, *89*, 98–105. [[CrossRef](#)]
48. Rodgers, C.J.; Blanford, C.F.; Giddens, S.R.; Skamnioti, P.; Armstrong, F.A.; Gurr, S.J. Designer laccases: A vogue for high-potential fungal enzymes? *Trends Biotechnol.* **2010**, *28*, 63–72. [[CrossRef](#)] [[PubMed](#)]
49. Balakshin, M.Y.; Chen, C.; Gratzl, J.S.; Kirkman, A.G.; Jakob, H. Kinetic studies on oxidation of veratryl alcohol by laccase-mediator system. Part 1. Effects of mediator concentration. *Holzforschung* **2000**, *54*, 165–170. [[CrossRef](#)]
50. Balakshin, M.Y.; Chen, C.; Gratzl, J.S.; Kirkman, A.G.; Jakob, H. Kinetic studies on oxidation of veratryl alcohol by laccase-mediator system. Part 2. The kinetics of dioxygen uptake. *Holzforschung* **2000**, *54*, 171–175. [[CrossRef](#)]
51. Solís-Oba, M.; Ugalde-Saldívar, V.M.; González, I.; Viniestra-González, G. An electrochemical–spectrophotometrical study of the oxidized forms of the mediator 2,2'-azino-bis-(3-ethylbenzothiazoline-6-sulfonic acid) produced by immobilized laccase. *J. Electroanal. Chem.* **2005**, *579*, 59–66. [[CrossRef](#)]
52. Potthast, A.; Rosenau, T.; Fischer, K. Oxidation of benzyl alcohols by the laccase-mediator system (LMS)—A comprehensive kinetic description. *Holzforschung* **2001**, *55*, 47–56. [[CrossRef](#)]
53. Fabbrini, M.; Galli, C.; Gentili, P. Comparing the catalytic efficiency of some mediators of laccase. *J. Mol. Catal. B Enzym.* **2002**, *16*, 231–240. [[CrossRef](#)]
54. Dong, S.; Xiao, H.; Huang, Q.; Zhang, J.; Mao, L.; Gao, S. Graphene facilitated removal of labetalol in laccase-ABTS system: Reaction efficiency, pathways and mechanism. *Sci. Rep.* **2016**, *6*, 21396. [[CrossRef](#)] [[PubMed](#)]
55. Krainer, F.W.; Glieder, A. An updated view on horseradish peroxidases: Recombinant production and biotechnological applications. *Appl. Microbiol. Biotechnol.* **2015**, *99*, 1611–1625. [[CrossRef](#)] [[PubMed](#)]
56. Shigeto, J.; Tsutsumi, Y. Diverse functions and reactions of class III peroxidases. *New Phytol.* **2016**, *209*, 1395–1402. [[CrossRef](#)] [[PubMed](#)]
57. Sterjiades, R.; Dean, J.F.D.; Eriksson, K.-E.L. Laccase from sycamore maple (*Acer pseudoplatanus*) polymerizes monolignols. *Plant Physiol.* **1992**, *99*, 1162–1168. [[CrossRef](#)] [[PubMed](#)]
58. Collins, P.J.; Dobson, A.D.W.; Field, J.A. Reduction of the 2,2'-azinobis(3-ethylbenzthiazoline-6-sulfonate) cation radical by physiological organic acids in the absence and presence of manganese. *Appl. Environ. Microbiol.* **1998**, *64*, 2026–2031. [[PubMed](#)]
59. Ahmed, F.; Dewani, R.; Pervez, M.K.; Mahboob, S.J.; Soomro, S.A. Non-destructive FT-IR analysis of mono azo dyes. *Bulg. Chem. Commun.* **2016**, *48*, 71–77.
60. Awale, A.G.; Ghose, S.B.; Utale, P.S. Synthesis, spectral properties and applications of some mordant and disperse mono azo dyes derived from 2-amino-1,3-benzothiazole. *Res. J. Chem. Sci.* **2013**, *3*, 81–87.
61. Dinçalp, H.; Toker, F.; Durucasu, I.; Avcıbaşı, N.; İcli, S. New thiophene-based azo ligands containing azo methine group in the main chain for the determination of copper(II) ions. *Dyes Pigments* **2007**, *75*, 11–24. [[CrossRef](#)]
62. Masoud, M.S.; Khalil, E.A.; Hindawya, A.M.; Ali, A.E.; Mohamed, E.F. Spectroscopic studies on some azo compounds and their cobalt, copper and nickel complexes. *Spectrochim. Acta. A Mol. Biomol. Spectrosc.* **2004**, *60*, 2807–2817. [[CrossRef](#)] [[PubMed](#)]
63. Yuen, C.W.M.; Ku, S.K.A.; Choi, P.S.R.; Kan, C.W.; Tsang, S.Y. Determining functional groups of commercially available ink-jet printing reactive dyes using Infrared Spectroscopy. *Res. J. Text. Appar.* **2005**, *9*, 26–38. [[CrossRef](#)]
64. Xu, F.; Shin, W.; Brown, S.H.; Wahleithner, J.A.; Sundaram, U.A.; Solomon, E.I. A study of a series of recombinant fungal laccases and bilirubin oxidase that exhibit significant differences in redox potential, substrate specificity, and stability. *Biochim. Biophys. Acta.* **1996**, *1292*, 303–311. [[CrossRef](#)]
65. Liu, H.; Zhou, P.; Wu, X.; Sun, J.; Chen, S. Radical scavenging by acetone: A new perspective to understand Laccase/ABTS inactivation and to recover redox mediator. *Molecules* **2015**, *20*, 19907–19913. [[CrossRef](#)] [[PubMed](#)]
66. Schnitzer, M.; Monreal, C.M.; Powell, E.E. Wheat straw biomass: A resource for high-value chemicals. *J. Environ. Sci. Health. B* **2014**, *49*, 51–67. [[CrossRef](#)] [[PubMed](#)]

67. Kenten, R.H.; Mann, P.J.G. The oxidation of manganese by peroxidase systems. *Biochem. J.* **1950**, *46*, 67–73. [[CrossRef](#)] [[PubMed](#)]
68. Christensen, N.J.; Kepp, K.P. Setting the stage for electron transfer: Molecular basis of ABTS-binding to four laccases from *Trametes versicolor* at variable pH and protein oxidation state. *J. Mol. Catal. B Enzym.* **2014**, *100*, 68–77. [[CrossRef](#)]
69. Enguita, F.J.; Marçal, D.; Martins, L.O.; Grenha, R.; Henriques, A.O.; Lindley, P.F.; Carrondo, M.A. Substrate and dioxygen binding to the endospore coat laccase from *Bacillus subtilis*. *J. Biol. Chem.* **2004**, *279*, 23472–23476. [[CrossRef](#)] [[PubMed](#)]
70. Bertin, C.; Yang, X.; Weston, L.A. The role of root exudates and allelochemicals in the rhizosphere. *Plant Soil* **2003**, *256*, 67–83. [[CrossRef](#)]
71. Neumann, G.; Bott, S.; Ohler, M.A.; Mock, H.-P.; Lippmann, R.; Grosch, R.; Smalla, K. Root exudation and root development of lettuce (*Lactuca sativa* L.cv.Tizian) as affected by different soils. *Front. Microbiol.* **2014**, *5*, 2. [[CrossRef](#)] [[PubMed](#)]
72. Liu, Y.-R.; Li, W.-G.; Chen, L.-F.; Xiao, B.-K.; Yang, J.-Y.; Yang, L.; Zhang, C.-G.; Huang, R.-Q.; Dong, J.-X. ABTS+ scavenging potency of selected flavonols from *Hypericum perforatum* L. by HPLC-ESI/MS QQQ: Reaction observation, adduct characterization and scavenging activity determination. *Food Res. Int.* **2014**, *58*, 47–58. [[CrossRef](#)]
73. Brausam, A.; Eigler, S.; Jux, N.; Van Eldik, R. Mechanistic investigations of the reaction of an iron(III) octa-anionic porphyrin complex with hydrogen peroxide and the catalyzed oxidation of diammonium-2,2'-azinobis(3-ethylbenzothiazoline-6-sulfonate). *Inorg. Chem.* **2009**, *48*, 7667–7678. [[CrossRef](#)] [[PubMed](#)]
74. Labrinea, E.P.; Georgiou, C.A. Stopped-flow method for assessment of pH and timing effect on the ABTS total antioxidant capacity assay. *Anal. Chim. Acta* **2004**, *526*, 63–68. [[CrossRef](#)]



© 2017 by the author. Licensee MDPI, Basel, Switzerland. This article is an open access article distributed under the terms and conditions of the Creative Commons Attribution (CC BY) license (<http://creativecommons.org/licenses/by/4.0/>).